

# Hadron calorimeter with MAPD readout in the NA61/SHINE experiment

A. Ivashkin<sup>a</sup>, F. Akhmadov<sup>b</sup>, R. Asfandiyarov<sup>c</sup>, A. Bravar<sup>c</sup>, A. Blondel<sup>c</sup>, W. Dominik<sup>d</sup>, Z. Fodor<sup>e</sup>, M. Gazdzicki<sup>f</sup>, M. Golubeva<sup>a</sup>, F. Guber<sup>a</sup>, A. Hasler<sup>c</sup>, A. Korzenev<sup>c</sup>, S. Kuleshov<sup>g</sup>, A. Kurepin<sup>a</sup>, A. Laszlo<sup>e</sup>, V. Marin<sup>a</sup>, Yu. Musienko<sup>a</sup>, O. Petukhov<sup>a</sup>, D. Röhrich<sup>h</sup>, A. Sadovsky<sup>a</sup>, Z. Sadygov<sup>b</sup>, T. Tolyhi<sup>e</sup>, F. Zerrouk<sup>i</sup>

<sup>a</sup>Institute for Nuclear research RAS, 117312 Moscow, Russia

<sup>b</sup>Joint Institute for Nuclear research RAS, Dubna, Russia

<sup>c</sup>University of Geneva, Switzerland

<sup>d</sup>Faculty of Physics, University of Warsaw, Warsaw, Poland

<sup>e</sup>KFKI Research Institute for Particle and Nuclear Physics, Budapest, Hungary

<sup>f</sup>Universities of Frankfurt and Kielce

<sup>g</sup>The Universidad Tecnica Federico Santa Maria, Valparaiso, Chile

<sup>h</sup>University of Bergen, Bergen, Norway

<sup>i</sup>Zecotek Imaging Systems Pte. Ltd., Singapore

## Abstract

The modular hadron calorimeter with micro-pixel avalanche photodiodes readout for the NA61/SHINE experiment at the CERN SPS is presented. The calorimeter consists of 44 independent modules with lead-scintillator sandwich structure. The light from the scintillator tiles is captured by and transported with WLS-fibers embedded in scintillator grooves. The construction provides a longitudinal segmentation of the module in 10 sections with independent MAPD readout. MAPDs with pixel density of  $10^4/\text{mm}^2$  ensure good linearity of calorimeter response in a wide dynamical range. The performance of the calorimeter prototype in a beam test is reported.

*Key words:* calorimeters, photodetectors, micro-pixel avalanche photodiodes

*PACS:* 29.40.Mc, 29.40.Wk, 29.40.Wj

## 1. Introduction

The goal of the NA61/SHINE experiment at CERN [1] is the search for the critical end-point and the onset of deconfinement in ion-ion collisions. A two dimensional scan of the phase diagram of strongly interacting matter will be done by changing the ion beam energy at the SPS (13-158 AGeV) and the size of the colliding systems. The critical point would be indicated by a maximum in the fluctuation of the particle multiplicity and other physical observables. The onset of deconfinement is revealed by rapid changes in the hadron production properties. Study of fluctuations due to properties of strongly interacting matter requires a very precise control over fluctuations caused by the variation of the number of interacting nucleons. The latter result from "trivial" event-by-event changes of the collision geometry. The number of interacting nucleons can be determined by measurements of the number of non-interacting nucleons from projectile nuclei (projectile spectators) by a very forward hadron calorimeter. The designed calorimeter for the NA61/SHINE experiment is called the Projectile Spectator Detector (PSD). Basic design requirements are good energy resolution,  $\frac{\sigma_E}{E} < \frac{60\%}{\sqrt{E(\text{GeV})}}$ , and good transverse uniformity of this resolution. Fully compensating modular lead/scintillator hadron calorimeters [2, 3] meet these requirements.

## 2. Calorimeter construction

The PSD calorimeter consists of 44 modules which cover a transverse area of  $120 \times 120 \text{ cm}^2$ . Each module consists of 60 lead/scintillator layers with 16 mm and 4 mm thickness, respectively. The lead/scintillator plates are tied together with 0.5 mm thick steel tape and placed in a box made of 0.5 mm thick steel. Steel tape and box are spot-welded together providing appropriate mechanical rigidity. The full length of modules corresponds to 5.7 nuclear interaction lengths. To fit the PSD transverse dimensions to the size of the spectator spots the distance between the NA61 target and the calorimeter is increased with increasing collision energy from 17 m to 23 m.

The central part of the PSD consists of 16 small modules with transverse dimension of  $10 \times 10 \text{ cm}^2$  and weight 120 kg each. Such fine transverse segmentation decreases the spectator occupancy in one module and improves the reconstruction of the reaction plane. The outer part of PSD the comprises 28 larger  $20 \times 20 \text{ cm}^2$  modules with a weight of 500 kg each. The mechanical rigidity of these heavy modules was enhanced by a slight modification of their structure. Namely, one 16 mm lead layer in the middle of the module was replaced by a steel plate with similar nuclear interaction length.

Light read-out is provided by Kyraray Y11 WLS-fibers embedded in round grooves in the scintillator plates. The WLS-fibers from each 6 consecutive scintillator tiles are collected together in a single optical connector at the end of the module.

Each of the 10 optical connectors at the downstream face of the module is read-out by a single photo-diode. The longitudinal segmentation into 10 sections ensures good uniformity of light collection along the module and delivers information on the type of particle which caused the observed particle shower. 10 photodetectors per module are placed at the rear side of the module together with the front-end-electronics.

### 3. Choice of photodetectors

Longitudinal segmentation of calorimeter modules requires 10 individual photodetectors per module for the signal read-out. Silicon photomultipliers SiPMs or micro-pixel avalanche photodiodes, MAPDs [4] are an optimum choice due to their remarkable properties such as high internal gain, compactness, low cost and immunity to the nuclear counter effect. Moreover, calorimetry applications have some specific requirements such as large dynamical range and linearity of photodetector response to intense light pulses. As known, the dynamic range and linearity of MAPDs are limited by the finite number of pixels. Most of the existing types of MAPDs with individual surface resistors have a pixel density  $10^3$  pixels/mm<sup>2</sup>. Such a limited number leads to a serious restriction of MAPD application in calorimetry, where the number of detected photons is comparable and even larger than the pixel number. The effect of saturation, when a few photons hit the same pixel, leads to significant non-linear MAPD response to light pulses with high intensity. Evidently, the MAPD has linear response only if the number of pixels is much larger than the number of incident photons. This feature represents a disadvantage of MAPDs compared to the traditional PMTs. However, this drawback is essentially reduced for MAPDs with individual micro-well structure [4], where a pixel density of  $10^4$ /mm<sup>2</sup> and higher is achievable. The above considerations motivated the choice of photodetectors: photodiodes of MAPD-3A type produced by Zecotek Photonics Inc. (Singapore) [5] were selected for the readout of the PSD hadron calorimeter. These MAPDs have a pixel density of 15000/mm<sup>2</sup>. Their 3x3 mm<sup>2</sup> active area nicely fits the size of the WLS-fiber bunch from one longitudinal section of a PSD module and provides a total number of pixels of more than  $10^5$  in one photodetector.

The MAPD-3A photon detection efficiency (PDE) for Y11 WLS-fiber emission spectrum at 510 nm reaches 15% and is rather similar to PMT performance, see Fig. 1. The operation voltage for different samples of MAPD-3A ranges from 65 V to 68 V. The maximum achieved gain is  $5 \times 10^4$ , see Fig. 2.

Since the PSD calorimeter has no beam hole to ensure maximum acceptance for the spectators, the central part of the PSD will be irradiated by the ion beam with an intensity up to  $10^5$  Hz. Therefore, one of the stringent requirements for the calorimeter readout is high count rate capability, at least in the central region. Here, the average amplitude in one longitudinal section of a PSD module is expected to be about 1500 photoelectrons. In other words, the recovery time of the selected MAPD-3A photodiode must be fast enough to ensure stable amplitudes at signal frequencies up to 100 kHz. To check the count rate capability of the MAPD-3A the dependence of its

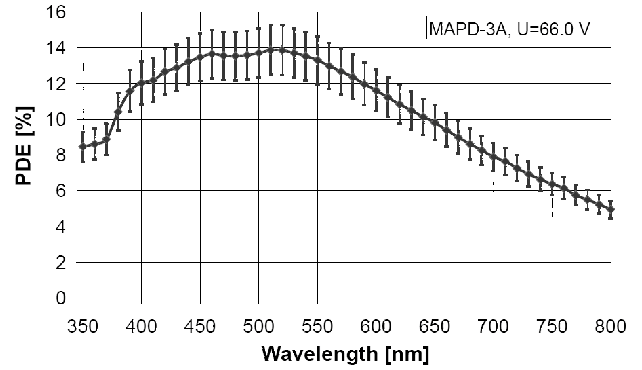


Figure 1: Spectral response of MAPD-3A: dependence of the photon detection efficiency PDE on the wavelength of light. The error bars correspond to the systematic uncertainty.

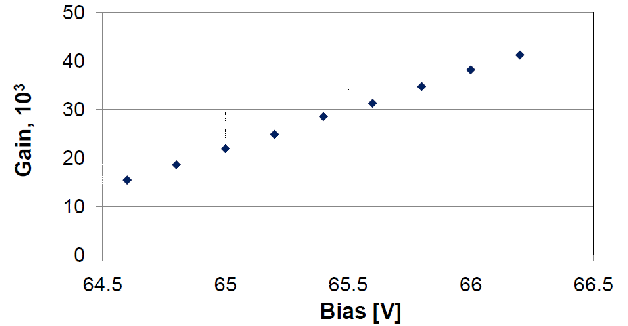


Figure 2: Dependence of MAPD-3A gain on the bias voltage.

amplitude on the frequency of light pulses was measured. The stability of the amplitude of the pulses at different frequencies from light emitting diode was checked by a normal PMT. The obtained behavior is presented in Fig. 3. As seen, the MAPD-3A amplitude would drop about 5% for the maximum beam intensity foreseen in the NA61/SHINE experiment.

To check the photodetector linearity measurements of MAPD amplitudes were performed with light pulses of different intensity. The number of incident photons was determined by a reference photodiode with known quantum efficiency and gain equal to one. The dependence of the MAPD amplitude on the number of incident photons is shown in Fig. 4. As seen, MAPD linearity is preserved for light pulses with a number of photons up to  $6 \times 10^4$ . Taking into account the photon detection efficiency of about 25% for the tested MAPD (with higher photon detection efficiency, but with the same pixel density as the MAPD-3A type) linear response to amplitudes up to 15000 photoelectrons is expected.

The reported comprehensive studies confirm that the selected MAPD-3A photodetectors satisfy the requirements of the NA61/SHINE experiment. At present, 320 MAPD-3A samples are installed in the available PSD modules and show stable operation during two months of calibration and beam technical beam runs.

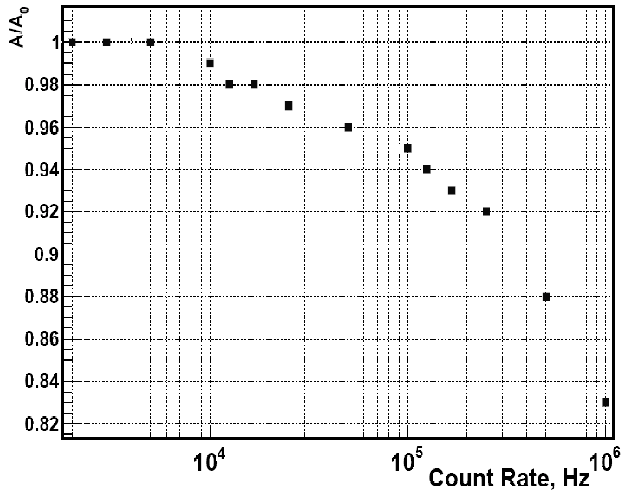


Figure 3: Dependence of normalized MAPD-3A amplitude on the frequency of light pulses with fixed intensity. The MAPD-3A amplitude at the frequency 1 kHz corresponds to 1500 photoelectrons.

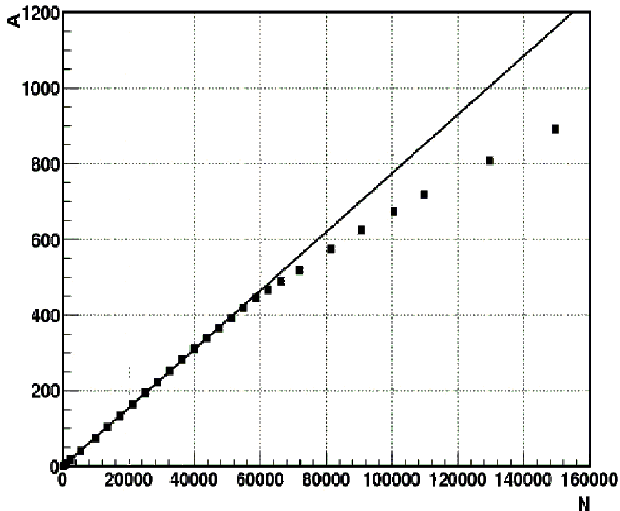


Figure 4: The dependence of MAPD amplitude (in relative units) on the number of incident photons.

#### 4. Beam tests of the PSD calorimeter

At present, the major part (16 small and 16 large modules) of the PSD calorimeter is assembled and installed in the NA61 experimental area. The construction of the full detector will be completed during the coming months. To check the performance of the calorimeter several tests using hadron beams at various energies were performed. For this purpose a PSD module array of nine small modules ( $3 \times 3$  array) was assembled. The first test at high energies was done in the NA61 H2 beam-line at the CERN SPS. The second test with low energy beams was carried out in the T10 beam-line at the CERN PS. The hadron beam energy ranged from 20 GeV to 158 GeV during the SPS test, and from 1 GeV to 6 GeV during the PS test. In both tests the calibration of all read-out channels was performed with a muon beam. In order to derive the full set of 90

calibration coefficients a muon beam scan was performed for all 9 modules and for 10 longitudinal sections in each module. The energy resolution of the central module of the tested array was estimated from data taken with hadron beams. Note, that the SPS hadron beam at low energies contains a significant fraction of muons and positrons. The spectrum of deposited energy in the first section of the central module exposed to the 30 GeV beam is shown in Fig. 5. The right-side peak in the

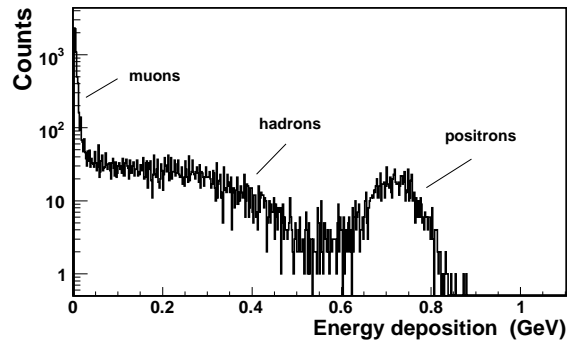


Figure 5: Energy spectrum measured in the first section of the central module for a 30 GeV hadron beam containing a fraction of muons and positrons.

spectrum corresponds to full positron energy absorption in the first longitudinal section that might be regarded as an electromagnetic calorimeter with rough sampling. The energy resolution for positrons at 30 GeV is about 6.5%.

The dependence of measured energy resolution on the pion energy is shown in Fig. 6. The tested prototype with  $30 \times 30$  cm<sup>2</sup> transverse size is too small to contain the entire hadron shower. Therefore, a non-negligible lateral shower leakage is expected. Monte Carlo simulations confirm that about 16% of hadron shower energy escapes from the tested array. The influence of shower leakage on the energy resolution was considered in [6, 7], where a third term in addition to the stochastic and constant ones was added in the parameterization of the resolution. The fit of the experimental data with the three-term formula (Fig. 6) gives the coefficient of the stochastic term equal to 56.1% and of the constant term equal to 2.1% at the fixed leakage term of 16%. A non-zero constant term might indicate that the selected lead/scintillator sampling does not provide full compensation. In order to reduce the lateral shower leakage a beam test of the calorimeter with a larger size will be performed soon.

The authors thank all members of the NA61/SHINE collaboration for fruitful discussions and permanent attention. This work was supported by the Polish Ministry of Science and Higher Education (grant PBP 2878/B/H03/2010/38), the Russian Foundation for Basic Research (grant 09-02-00664), Cooperation Programme Switzerland-Russia (grant STCP-RUSSIA/S17604) and by FONDECYT (Chile) under the project 1100582 and Centro-Científico-Tecnológico de Valparaíso PBCT ACT-028.

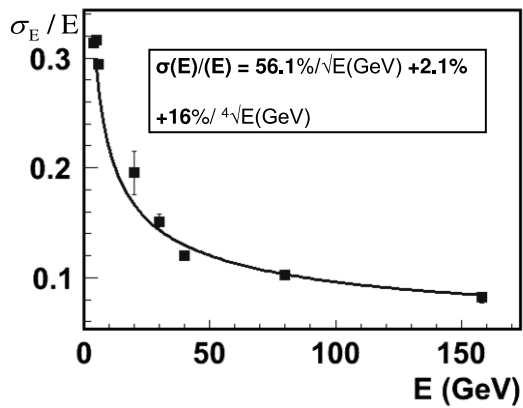


Figure 6: The energy resolution of the tested PSD prototype as a function of hadron beam energy . The solid line is the fit of experimental data by the function shown in the insert.

## References

- [1] N. Antoniou et al. [NA49-future Collaboration], SPSC-P-330; CERN-SPSC-2006-034. The NA61/SHINE homepage[<http://na61.web.cern.ch>].
- [2] G. A. Alekseev et al., Nucl. Instr. and Meth. A **461**, 381 (2001).
- [3] Y. Fujii, Nucl. Instr. and Meth. A **453**, 237 (2000).
- [4] Z. Sadygov et al., Nucl. Instr. and Meth. A **567**, 70 (2006).
- [5] The Zecotek homepage[<http://zecotek.com>].
- [6] D. Acosta et al., Nucl. Instr. and Meth. A **308**, 481 (1991).
- [7] J. Badier et al., Nucl. Instr. and Meth. A **337**, 326 (1994).